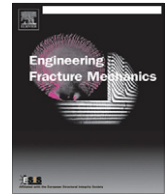




ELSEVIER

Contents lists available at ScienceDirect

## Engineering Fracture Mechanics

journal homepage: [www.elsevier.com/locate/engfracmech](http://www.elsevier.com/locate/engfracmech)

## A two scale anisotropic damage model accounting for initial stresses in microcracked materials

S. Levasseur<sup>a</sup>, F. Collin<sup>a</sup>, R. Charlier<sup>b</sup>, D. Kondo<sup>c,\*</sup>

<sup>a</sup> FRS-FNRS, Université de Liège (ULg) Chemin des Chevreuils, 1, 4000 Liège, Belgium

<sup>b</sup> Université de Liège (ULg), Chemin des Chevreuils, 1, 4000 Liège, Belgium

<sup>c</sup> Université Pierre et Marie Curie (UPMC), Institut d'Alembert, 4 place Jussieu, 75005 Paris, France

### ARTICLE INFO

#### Article history:

Received 19 April 2010

Received in revised form 25 February 2011

Accepted 18 March 2011

Available online xxx

#### Keywords:

Anisotropic damage

Initial stresses

Homogenization

Micromechanics

Geomaterials

Microcracked media

### ABSTRACT

In a recent study [15], we proposed a class of isotropic damage models which account for initial stresses. The present paper extends this approach to anisotropic damage due to growth of an arbitrarily penny-shaped microcracks system. The basic principle of the upscaling technique in the presence of initial stress is first recalled. Then, we derive a closed-form expression of the elastic energy potential corresponding to a system of arbitrarily oriented microcracks. It is shown that the coupling between initial stresses and damage is strongly dependent of the microcracks density and orientation. Predictions of the proposed model are illustrated through the investigation of the influence of initial stresses on the material response under non monotonous loading paths. Finally, by considering a particular distribution of microcracks orientation, described by a second order damage tensor, it is shown that the model is a generalization of the macroscopic damage model of Halm and Dragon [9], for which a physically-based interpretation is then proposed.

© 2011 Published by Elsevier Ltd.

### 1. Introduction

The mechanical behavior of engineering materials and in particular geomaterials is significantly affected by the presence of voids or crack-like defects. Modeling of such behavior is generally performed by considering purely macroscopic or micro-mechanically-based damage models (see for instance [1,9,21,12], etc.). Recent developments in homogenization of microcracked media provides now physical and mathematical models for the description of damage-induced anisotropy, as well as cracks closure effects ([23,24,7]). The above models have been applied for geomaterials including concrete or rock-like media [27]. However, except an interesting attempt to incorporate damage-induced residual stresses by Halm and Dragon [9] in the context of purely macroscopic modeling, most of the damage models proposed in literature do not directly account for in situ initial stresses, which are however crucial in geomechanics (tunneling, compaction of petroleum reservoir, waste storage). It is convenient to emphasize that pre-stresses in geotechnical problems can also originate from the loading conditions (gravity in most cases), and as such, should be handled at the macroscopic scale. In the present work, no attempt is done to account for these types of pre-stresses, which are different in nature from those introduced by means of homogenization techniques in the constitutive description.

In the perspective of the previously mentioned applications in geomechanics,<sup>1</sup> it is desirable to formulate a micromechanical anisotropic damage model which takes into account initial stresses and to determine how they affect the response of a

\* Corresponding author.

E-mail address: [djimedokondo@upmc.fr](mailto:djimedokondo@upmc.fr) (D. Kondo).

<sup>1</sup> Note that several other domains of applications require also a suitable consideration of initial stresses induced by the formation process. Damage in porous bone is also concerned (see [14]).

## Nomenclature

$\Omega$	representative elementary volume ( <i>rev</i> ) located at macroscopic point. Its boundary is $\partial\Omega$
$\Omega^s$	domain occupied by the solid matrix
$\Omega^I$	domain occupied by the inclusion $I$
$\varphi^r$	porosity of the $r$ th family of cracks
$\varphi$	total porosity of cracks; $1 - \varphi$ is then the solid volume fraction
$k^s$	elastic bulk modulus of the isotropic solid phase
$\mu^s$	elastic shear modulus of the isotropic solid phase
$E^s$	Young modulus of the isotropic solid phase
$\nu^s$	Poisson ratio of the isotropic solid phase
$d^r$	crack density parameter of the $r$ th cracks family; $\underline{d}$ denotes the set of these parameters for all cracks families
$\Psi$	potential of the microcracked material
$\mathcal{F}^{d^r}$	energy release rate; thermodynamic force associated to the $r$ th cracks family
$f^r$	damage yield function of the $r$ th cracks family
$\mathcal{R}(d^r)$	resistance to damage of the $r$ th cracks family; it is chosen as an affine function defined by two constants $h_0$ and $\nu^s$
$\underline{z}$	position vector at the microscopic scale
$\underline{n}^r$	normal vector to the $r$ th cracks family
$\omega^r$	weighting coefficient associated with unit normal $\underline{n}^r$
$S^2$	surface of the unit sphere
$\delta$	second order unit tensor
$\sigma(\underline{z})$	microscopic Cauchy stress tensor at point $\underline{z}$
$\Sigma$	macroscopic Cauchy stress tensor at point $\underline{x}$
$\sigma_0$	initial uniform Cauchy stress tensor in the solid
$\sigma^p$	heterogeneous prestress tensor field
$\varepsilon$	microscopic strain tensor at point $\underline{z}$
$\mathbf{E}$	macroscopic strain tensor at point $\underline{x}$
$\mathbf{D}$	macroscopic second order tensor of the approximate anisotropic damage model
$\mathbb{A}^r(\underline{z})$	strain localization tensor of phase $r$
$\mathbb{I}$	fourth order symmetric unit tensor
$\mathbb{J} = \frac{1}{3} \mathbf{1} \otimes \mathbf{1}$ and $\mathbb{K} = \mathbb{I} - \mathbb{J}$	fourth order projectors unit tensor
$\mathbb{C}^s$	elastic stiffness tensor of the solid
$\mathbb{C}^I$	elastic stiffness tensor of inclusion $I$
$\mathbb{C}^{hom}$	homogenized elastic stiffness tensor
$\mathbb{C}_{dil}^{hom}$	dilute estimate of the homogenized elastic stiffness tensor
$\mathbb{C}_t^{hom}$	homogenized elastic stiffness tensor
$\mathbb{S}^r$	Eshelby tensor of $r$ th family of cracks

material sustaining damage by cracks growth at small scale. Before presenting the specific developments carried out in the present study, it is convenient to note that although the use of the concept of prestress in the context of cracks-induced damage modeling with prestress is in several aspects original, various micromechanics-based models already exist in literature but they concern poroelastic damage, strength and/or poroplasticity (see for instance among others [8,2,7,18,15] and references cited herein).

The main purpose of the present study is to derive from homogenization techniques a new micro-macro anisotropic damage model which incorporates initial stresses and couples them to the evolving damage. The paper is organized as follows. We first present the basic principles of the micromechanical modeling, which is then applied to the case of an elastic matrix weakened by an arbitrary distribution of microcracks. The obtained result are then used for the formulation of the constitutive law for anisotropic microcracked media. Next, are presented examples that illustrate and highlight the role of prestresses on the material's response. Finally, on the basis of the above results, we formulate a simplified orthotropic damage model. Based on this model, a new physically-based interpretation of the macroscopic phenomenological model of [9] can be obtained.

## 2. Principle of the modeling including initial stresses

Consider a representative elementary volume (*REV*)  $\Omega$ , made up of a solid matrix  $s$  (occupying a domain  $\Omega^s$ ) and an arbitrary system of inhomogeneous inclusions; each inclusion family, denoted by  $I$ , occupies a domain  $\Omega^I$ . The matrix and the inclusions are considered to behave elastically. Moreover, an initial uniform stress field  $\sigma_0$  is assumed in the solid matrix. Let  $\underline{z}$  denotes the position vector,  $\underline{\xi}$  the displacement vector, and  $\mathbf{E}$  the macroscopic strain tensor. The *REV* is subjected, as classically, to uniform strain boundary conditions :

$$\text{on } \partial\Omega : \underline{\xi} = \mathbf{E} \cdot \underline{z} \quad (1)$$

A convenient way to formulate the homogenization problem with initial stresses in a unified way is to consider the stress tensor field  $\boldsymbol{\sigma}(\underline{z})$ , everywhere in the *REV*, in an affine form:

$$(\forall \underline{z} \in \Omega) \quad \boldsymbol{\sigma}(\underline{z}) = \mathbb{C}(\underline{z}) : \boldsymbol{\varepsilon}(\underline{z}) + \boldsymbol{\sigma}^p(\underline{z}) \quad (2)$$

where  $\mathbb{C}(\underline{z})$  is the heterogeneous stiffness, and  $\boldsymbol{\sigma}^p(\underline{z})$  a prestress tensor such as:

$$\mathbb{C}(\underline{z}) = \begin{cases} \mathbb{C}^I & \text{in}(\Omega^I) \\ \mathbb{C}^S & \text{in}(\Omega^S) \end{cases} \text{ and } \boldsymbol{\sigma}^p(\underline{z}) = \begin{cases} \boldsymbol{\sigma}_0 & \text{in}(\Omega^S) \\ \mathbf{0} & \text{in}(\Omega^I) \end{cases} \quad (3)$$

In this form, the problem can be solved by using the classical Levin's theorem [16] (see also [13]). This yields the following constitutive equation (see [7] in a general context of poroelasticity):

$$\boldsymbol{\Sigma} = \mathbb{C}^{hom} : \mathbf{E} + \overline{\boldsymbol{\sigma}^p} : \mathbb{A} \quad (4)$$

in which the overbar represents the average of any considered quantity over the *REV*. The fourth order tensor  $\mathbb{A}$  is the so-called heterogeneous strain localization tensor which relates the microscopic strain tensor and the macroscopic strain tensor  $\mathbf{E}$  in absence of initial stress:  $\boldsymbol{\varepsilon}(\underline{z}) = \mathbb{A}(\underline{z}) : \mathbf{E}$ . Tensor  $\mathbb{C}^{hom}$  represents the macroscopic stiffness tensor which can be obtained from any homogenization scheme in standard linear elasticity (e.g. without prestress), and,  $\boldsymbol{\Sigma}$  is the macroscopic stress (average over the *REV*), i.e.  $\boldsymbol{\Sigma} = \overline{\boldsymbol{\sigma}(\underline{z})}$ . Recalling that the prestress is null in  $\Omega^I$  and is equal to  $\boldsymbol{\sigma}_0$  in  $\Omega^S$ , it is readily seen that:

$$\boldsymbol{\Sigma} = \mathbb{C}^{hom} : \mathbf{E} + (1 - \varphi)\boldsymbol{\sigma}_0 : \mathbb{A}^S = \mathbb{C}^{hom} : \mathbf{E} + \boldsymbol{\sigma}_0 : \left( \mathbb{I} - \sum_{r=1}^N \varphi^r \mathbb{A}^r \right) \quad (5)$$

$\mathbb{A}^S$  is the average of concentration tensor over the solid matrix, while  $\mathbb{A}^r$  corresponds to the average value of the localization tensor of the  $r$ th family of inclusions. Since now these inclusions are cracks,  $\varphi = \sum_{r=1}^N \varphi^r$  denotes the total volume fraction of the cracks, i.e. the cracks porosity. Since  $\mathbb{C}^{hom} = \mathbb{C}^S : \left( \mathbb{I} - \sum_{r=1}^N \varphi^r \mathbb{A}^r \right)$ , (5) can be also put in the form:

$$\boldsymbol{\Sigma} = (\mathbb{C}^S : \mathbf{E} + \boldsymbol{\sigma}_0) : \left( \mathbb{I} - \sum_{r=1}^N \varphi^r \mathbb{A}^r \right) \quad (6)$$

Note that the initial stress simply combines with  $\mathbb{C}^S : \mathbf{E}$  in the expression of the macroscopic stress of the heterogeneous material.

### 3. Theoretical formulation of anisotropic damage model with account for initial stresses

We still consider a *REV* composed of an elastic matrix containing penny-shaped cracks. The matrix is submitted to the uniform initial stress  $\boldsymbol{\sigma}_0$  and at its exterior boundary to an uniform strain. The aim here is to derive a simple model of elastic damage due to cracks growth. To this end, the localization tensor  $\mathbb{A}^r$  corresponding to the  $r$ th family of cracks is required. It depends on the considered homogenization scheme. Due to the matrix/inclusion morphology studied here and to reduce the complexity of the resulting anisotropic damage model, as a first attempt we will adopt a dilute homogenization scheme.

#### 3.1. Overall potential of the microcracked medium in the presence of initial stress: the case of a dilute approximation

The localization tensor corresponding to the dilute scheme reads:

$$\mathbb{A}^r = \mathbb{A}_{dil}^r = (\mathbb{I} - \mathbb{S}^r)^{-1} \quad (7)$$

in which  $\mathbb{S}^r$  is the Eshelby tensor whose expression for penny-shaped cracks can be found in [11] or in [20].

Following a dilute scheme-based approach of penny-shaped cracks (considered as spheroid with very low aspect ratio) (see for instance [11] or [7]), it can be shown that:

$$\boldsymbol{\Psi}(\mathbf{E}, \underline{d}) = \frac{1}{2} \mathbf{E} : \mathbb{C}_{dil}^{hom}(\underline{d}) : \mathbf{E} + \boldsymbol{\sigma}_0 : \mathbf{E} - \frac{4}{3} \pi \boldsymbol{\sigma}_0 : \left( \sum_{r=1}^N d^r \mathbb{T}^r \right) : \mathbf{E} \quad (8)$$

with

$$\mathbb{T}^r = \lim_{X_r \rightarrow 0} X_r (\mathbb{I} - \mathbb{S}^r)^{-1} \quad (9)$$

$X_r$  and  $a^r$  being the aspect ratio and radius of cracks belonging to the  $r$ th family, respectively.  $|\Omega|$  being the volume of the *REV*, the quantity  $d^r = \frac{(a^r)^3}{|\Omega|}$  represents the cracks density parameter already introduced by Budiansky and O'Connell [5]. Note that the dilute estimate of the macroscopic stiffness tensor reads:

$$\mathbb{C}_{dil}^{hom} = \mathbb{C}^S : \left( \mathbb{I} - \frac{4\pi}{3} \sum_{r=1}^N d^r \mathbb{T}^r \right) \quad (10)$$

Let us consider now an isotropic elastic matrix whose stiffness is given by:

$$\mathbb{C}^s = 3k^s \mathbb{J} + 2\mu^s \mathbb{K} \quad (11)$$

with  $\mathbb{J} = \frac{1}{3} \delta \otimes \delta$ ,  $\mathbb{K} = \mathbb{I} - \mathbb{J}$ , tensor  $\mathbb{I}$  being the symmetric fourth order unit tensor and  $\delta$  the second order unit tensor. The scalars  $k^s = \frac{E^s}{3(1-2\nu^s)}$  and  $\mu^s = \frac{E^s}{2(1+\nu^s)}$  are the bulk modulus and the shear modulus of the solid matrix, respectively.  $E^s$  is its Young modulus while  $\nu^s$  is the Poisson ratio. For any given cracks family,  $r$ , whose unit normal is denoted  $\underline{n}^r$ :

$$\mathbb{T}^r = \frac{4(1-\nu^s)}{\pi} \left[ \frac{\nu^s}{1-2\nu^s} (\underline{n}^r \otimes \underline{n}^r) \otimes \delta + \frac{1}{2-2\nu^s} [\delta \otimes (\underline{n}^r \otimes \underline{n}^r) + (\underline{n}^r \otimes \underline{n}^r) \otimes \delta] - \frac{\nu^s}{2-2\nu^s} \underline{n}^r \otimes \underline{n}^r \otimes \underline{n}^r \otimes \underline{n}^r \right] \quad (12)$$

where for any second order tensors  $\mathbf{a}$  and  $\mathbf{b}$ , the components of the symmetric fourth order tensor  $\mathbf{a} \otimes \mathbf{b}$  are  $(\mathbf{a} \otimes \mathbf{b})_{ijkl} = \frac{1}{2} (a_{ik} b_{jl} + a_{il} b_{jk})$ .

It is readily seen that the dilute scheme-based estimate of the energy potential, given by (8), takes the form:

$$\Psi(\mathbf{E}, \underline{d}) = \frac{1}{2} \mathbf{E} : \mathbb{C}_{dil}^{hom}(\underline{d}) : \mathbf{E} + \boldsymbol{\sigma}_0 : \mathbf{E} - \frac{16}{3} (1-\nu^s) \boldsymbol{\sigma}_0 : \sum_{r=1}^N \left[ \mathcal{A}^r d^r \underline{n}^r \otimes \underline{n}^r + \frac{2}{2-\nu^s} d^r (\underline{n}^r \otimes \underline{n}^r) \cdot \mathbf{E} \right] \quad (13)$$

with the scalar  $\mathcal{A}^r$  expressed as:

$$\mathcal{A}^r = \frac{\nu^s}{1-2\nu^s} tr \mathbf{E} - \frac{\nu^s}{2-\nu^s} tr(\mathbf{E} \cdot (\underline{n}^r \otimes \underline{n}^r)) \quad (14)$$

It is interesting to point out that the couplings between initial stresses, damage and deformation state contain terms of different nature:

- a standard coupling between initial stresses  $\boldsymbol{\sigma}_0$  and macroscopic deformation, as in classical linear elasticity with pre-stress:  $\boldsymbol{\sigma}_0 : \mathbf{E}$ ,
- a *weak* coupling between  $\boldsymbol{\sigma}_0$ , damage and deformation; the weakness of this coupling lies in the occurrence of macroscopic strain tensor  $\mathbf{E}$  only through the scalar quantity  $\mathcal{A}^r$ ,
- a strong coupling between initial stresses  $\boldsymbol{\sigma}_0$ , and both damage and deformation state through the term  $\boldsymbol{\sigma}_0 : [(d^r \underline{n}^r \otimes \underline{n}^r) \cdot \mathbf{E}]$ .

Accordingly, for the microcracked material, the state law giving the macroscopic stress tensor,  $\boldsymbol{\Sigma} = \frac{\partial \Psi(\mathbf{E}, \underline{d})}{\partial \mathbf{E}}$ , derived from (13), reads:

$$\boldsymbol{\Sigma} - \boldsymbol{\sigma}_0 = \mathbb{C}^{hom} : \mathbf{E} - \frac{16}{3} (1-\nu^s) \boldsymbol{\sigma}_0 : \sum_{r=1}^N \left[ \frac{\nu^s}{1-2\nu^s} \delta \otimes (d^r \underline{n}^r \otimes \underline{n}^r) - \frac{\nu^s}{2-\nu^s} d^r \underline{n}^r \otimes \underline{n}^r \otimes \underline{n}^r \otimes \underline{n}^r \right] - \frac{32(1-\nu^s)}{3(2-\nu^s)} \sum_{r=1}^N \boldsymbol{\sigma}_0 \cdot (d^r (\underline{n}^r \otimes \underline{n}^r)) \quad (15)$$

### 3.2. Damage yield function and rate form of the anisotropic damage law

It is first convenient to point out that the set of scalar microcracks density parameters  $\underline{d} = \{d^r, r = 1-N\}$  defines the damage variables corresponding to the considered microcracks system whose evolution law is required for the formulation of the damage model. In order to establish the damage evolution law, we follow the standard thermodynamics-based approach (see for instance [19]) consisting in a careful analysis of the mechanical dissipation. In this framework, the damage yield function is written by considering the thermodynamical force  $F^{d^r}$  associated to each  $d^r$  (obtained as the negative of the derivative of  $\Psi$  with respect to  $d^r$ ):

$$\mathcal{F}^{d^r} = -\frac{\partial \Psi}{\partial d^r} = -\frac{1}{2} \mathbf{E} : \frac{\partial \mathbb{C}^{hom}}{\partial d^r} : \mathbf{E} + \frac{16}{3} (1-\nu^s) \boldsymbol{\sigma}_0 : \left[ \mathcal{A}(\mathbf{E}, \underline{n}^r) \underline{n}^r \otimes \underline{n}^r + \frac{2}{2-\nu^s} (\underline{n}^r \otimes \underline{n}^r) \cdot \mathbf{E} \right] \quad (16)$$

Note that, due to the consideration of a dilute scheme,  $\mathcal{F}^{d^r}$  does not depend on the microcrack density parameter  $d^r$ .

The following damage criterion is then proposed:

$$f^r(\mathcal{F}^{d^r}, \underline{d}) = \mathcal{F}^{d^r} - \mathcal{R}(d^r) \leq 0 \quad (17)$$

where  $\mathcal{R}(d^r)$  is the local resistance to damage propagation.

By assuming a damage normality rule, the damage evolution law reads:

$$\dot{d}^r = \frac{\left( \frac{\partial \mathcal{C}^{hom}}{\partial d^r} : \mathbf{E} - X^r \right) : \dot{\mathbf{E}}}{\mathcal{R}'(d^r)} \quad (18)$$

in which

$$X^r = \frac{16}{3}(1 - \nu^s)\sigma_0 : \left[ \frac{\nu^s}{1 - 2\nu^s}\delta \otimes (\underline{n}^r \otimes \underline{n}^r) - \frac{\nu^s}{2 - \nu^s}\underline{n}^r \otimes \underline{n}^r \otimes \underline{n}^r \otimes \underline{n}^r \right] + \frac{32}{3} \frac{1 - \nu^s}{2 - \nu^s} \sigma_0 \cdot (\underline{n}^r \otimes \underline{n}^r) \quad (19)$$

Eq. (18) together with (19) show that, in addition to modifying the damage yield function,  $\sigma_0$  also affects the rate of damage. The rate form of the constitutive damage law is then given by:

$$\dot{\Sigma} = \mathbb{C}_t^{hom} : \dot{\mathbf{E}} \quad (20)$$

with

$$\mathbb{C}_t^{hom} = \mathbb{C}^{hom} - \sum_{r=1}^N H^r \frac{\left( \frac{\partial \mathbb{C}_t^{hom}}{\partial d^r} : \mathbf{E} - X^r \right) \otimes \left( \frac{\partial \mathbb{C}_t^{hom}}{\partial d^r} : \mathbf{E} - X^r \right)}{\mathcal{R}'(d^r)} \quad (21)$$

where  $\mathcal{R}'(d^r)$  represents the derivative of  $\mathcal{R}$  with respect to  $d^r$ . Moreover, one has:

$$H^r = \begin{cases} 0 & \text{if } f^r < 0 \quad \text{or if } f^r = 0 \quad \text{and } \dot{f}^r < 0 \\ 1 & \text{if } f^r = 0 \quad \text{and } \dot{f}^r = 0 \end{cases} \quad (22)$$

In summary, note that the initial stress  $\sigma_0$  affects not only the state laws of the damaged material, but also the domain of elasticity predicted by the model (see the damage yield function), as well as the rate of damage and the corresponding tangent operator  $\mathbb{C}_t^{hom}$  (see (21)). It must be emphasized that  $\sigma_0$  affects the tangent operator through the quantity  $X_r$ .

Considering the specific expression of the damage threshold  $\mathcal{R}(d^r)$  in Eq. (17), we follow [19] and consider  $\mathcal{R}(d^r) = h_0(1 + \eta d^r)$ ,  $h_0$  and  $\eta$  being parameters of the model.

### 3.3. Damage modeling accounting for unilateral effects in presence of prestress

The aim of this subsection is to extend the previous modeling framework (see sub Sections 3.2 and 3.1) in order to account for unilateral effects due to microcracks closure, which can occur during some specific loading paths. Inspired by existing micromechanical modelings without prestress, for a family of microcracks  $r$ , the transition between opening and closure states occurs when the normal stress,  $\Sigma : (\underline{n}^r \otimes \underline{n}^r)$ , is equal to 0.

For closed microcracks, the computations are quite similar to the previous ones devoted to open cracks, except that in Eqs. (8) and (10) tensor  $\mathbb{T}^r$  is replaced by:

$$\mathbb{T}^{r*} = \frac{4(1 - \nu^s)}{\pi(2 - \nu^s)} [\delta \otimes (\underline{n}^r \otimes \underline{n}^r) + (\underline{n}^r \otimes \underline{n}^r) \otimes \delta - 2(\underline{n}^r \otimes \underline{n}^r) \otimes (\underline{n}^r \otimes \underline{n}^r)] \quad (23)$$

and consequently,  $\mathcal{A}^r$  and  $X^r$  are replaced in Eqs. (13), (16), (18) and (21) by:

$$\mathcal{A}^{r*} = -\frac{2}{2 - \nu^s} \text{tr}(\mathbf{E} \cdot (\underline{n}^r \otimes \underline{n}^r)) \quad (24)$$

and

$$X^{r*} = \frac{32}{3} \frac{1 - \nu^s}{2 - \nu^s} [\sigma_0 \cdot (\underline{n}^r \otimes \underline{n}^r) - \sigma_0 : (\underline{n}^r \otimes \underline{n}^r \otimes \underline{n}^r \otimes \underline{n}^r)] \quad (25)$$

Finally, the state law (15) becomes:

$$\Sigma - \sigma_0 = \mathbb{C}^{hom} : \mathbf{E} - \frac{32}{3} \frac{(1 - \nu^s)}{(2 - \nu^s)} \sum_{r=1}^N [\sigma_0 \cdot (d^r (\underline{n}^r \otimes \underline{n}^r)) - \sigma_0 : (d^r \underline{n}^r \otimes \underline{n}^r \otimes \underline{n}^r \otimes \underline{n}^r)] \quad (26)$$

## 4. Illustration of the capabilities of the anisotropic damage model with prestress

For the purpose of simple illustrations of the capabilities of the present dilute scheme-based model, we consider an uniaxial macroscopic tensile loading path ( $\Sigma = \Sigma \underline{e}_1 \otimes \underline{e}_1$ ) and an isotropic tensile initial stress field, ( $\sigma_0 = \sigma_0 \mathbf{1}$ ). The uniaxial tensile load induces anisotropic damage which are influenced by the initial stress  $\sigma_0$ . Simulations are performed with the following values for the material parameters: matrix Young modulus  $E^s = \frac{100}{3}$  GPa, Poisson ratio of the matrix  $\nu^s = 0.23$ . Parameters of the damage yield function are taken as  $h_0 = 10^4$  J/m<sup>2</sup> and  $\eta = 32$ .

Due to absence of data concerning the nature of the initial microcracking, we assume a randomly oriented distribution of microcracks. Therefore, the implementation of the anisotropic damage model requires an orientational average (integration) over the surface of unit sphere. This numerical implementation procedure is inspired from studies on microplane models [3] (see also [24] in the context of micromechanical damage models).

In Fig. 1 are presented the uniaxial stress–strain curves according to the model for different values of the initial stress  $\sigma_0$ . The axial strain is denoted  $E_{33}$ , while  $E_{11} = E_{22}$  corresponds to the radial strain. It is observed that the magnitude of  $\sigma_0$  has a

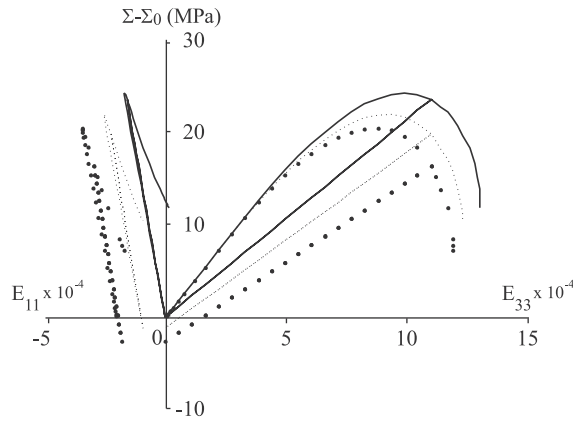


**Fig. 1.** Comparison of the predicted responses by the dilute scheme-based model for uniaxial loading with different levels of prestress (full line: zero prestress, dashed line: 5 MPa of prestress, dots: 10 MPa of prestress).

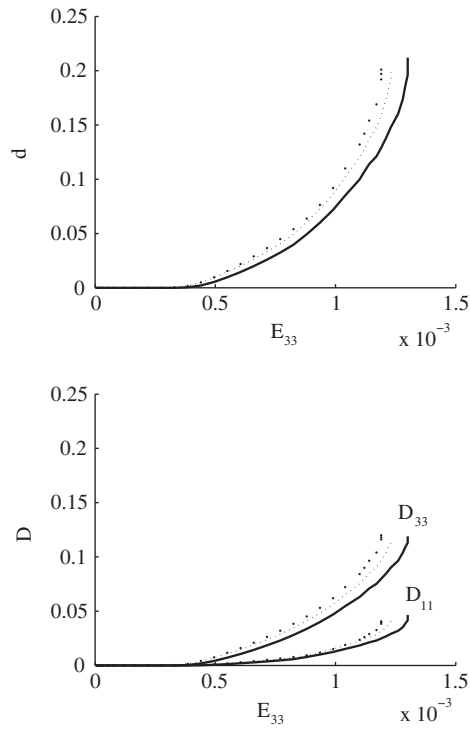


**Fig. 2.** Comparison of the damage according to the dilute scheme-based model for uniaxial loading for different levels of prestress (full line: zero prestress, dashed line: 5 MPa of prestress, dots: 10 MPa of prestress).

clear impact on the overall response of the material undergoing damage: yield stress, peak stress, stress–strain curve including softening regime are modified. A residual strain (corresponding to  $\Sigma - \sigma_0 = 0$ ), related to the state of the damage before unloading, is observed.

A simple and approximate representation of the damage state is given by the following second order tensor  $\mathbf{D}$ :

$$\mathbf{D} = \frac{1}{4\pi} \int_{S^2} d(\underline{n})(\underline{n} \otimes \underline{n}) dS \tag{27}$$

which can be discretized as:

$$\mathbf{D} = \sum_{r=1}^N \omega^r d^r \underline{n}^r \otimes \underline{n}^r \tag{28}$$

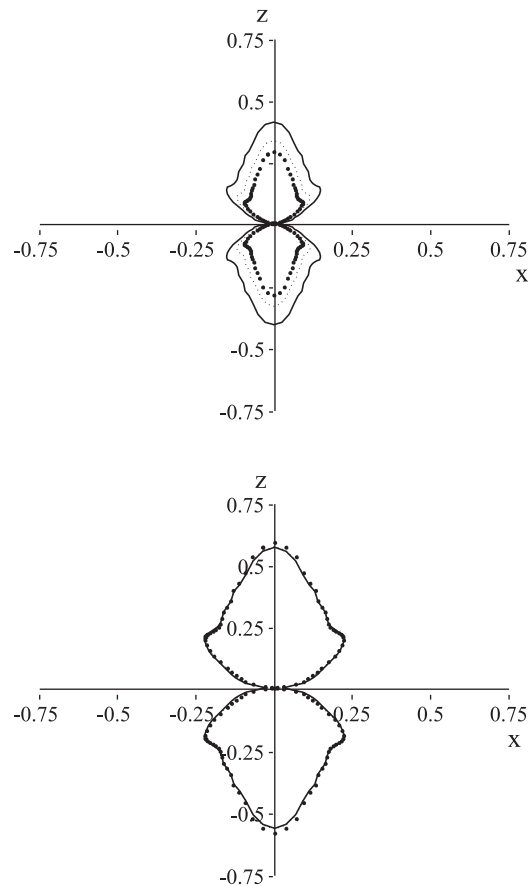


**Fig. 3.** Comparison of the damage orientational distribution according to the dilute scheme-based model for uniaxial loading (along z-axis) for different levels of prestress (full line: zero prestress, dashed line: 5;MPa of prestress, dots: 10 MPa of prestress).

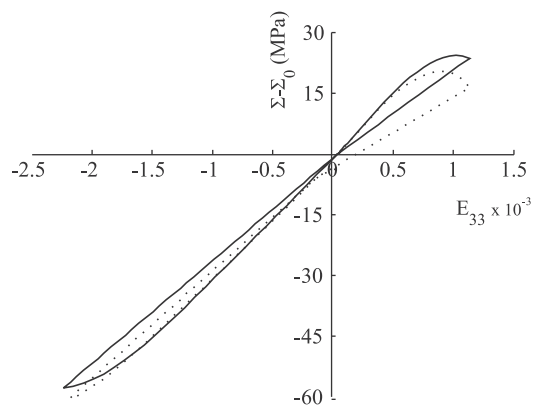


**Fig. 4.** Comparison of the responses according to the dilute scheme-based model for uniaxial loading for two different levels of prestress (full line: zero prestress, dots: 10 MPa of prestress).

in which  $\omega^r$  is the weighting coefficient associated with  $\underline{n}^r$ , the normal orientation of the  $r$ -crack. The integration domain,  $\mathcal{S}^2$ , is the surface of the unit sphere. The number  $N$  of integration orientations (and then the components of  $\underline{n}^r$ ) and the corresponding values of  $\omega^r$  strongly depend on the considered integration scheme. Previous studies (e.g. [24]) have shown that no significant difference in accuracy is obtained if 33 crack families are used rather than 21. The set of 21 families of microcracks are retained in the present work.

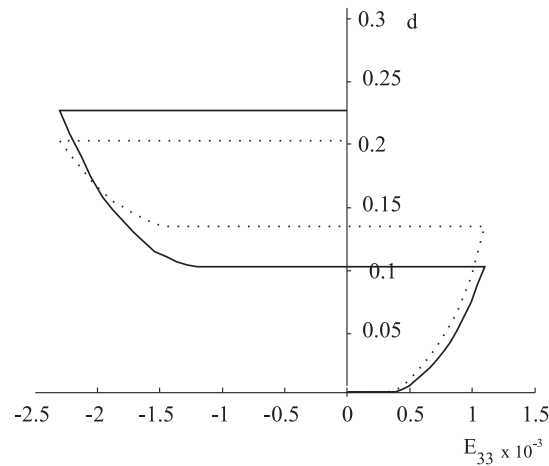


**Fig. 5.** Comparison of the damage according to the dilute scheme-based model for uniaxial loading (along  $z$ -axis) for two different levels of prestress (full line: zero prestress, dots: 10 MPa of prestress).

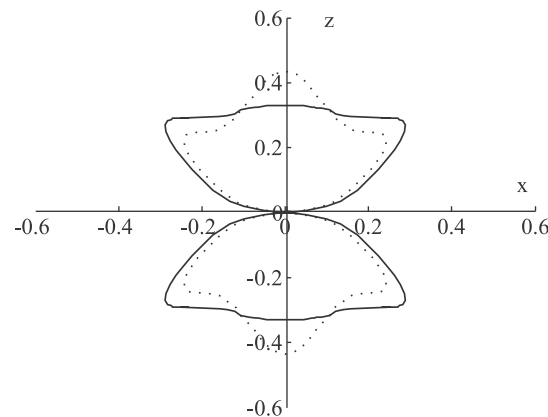


**Fig. 6.** Comparison of the damage orientational distribution according to the dilute scheme-based model for uniaxial loading (along  $z$ -axis) for two different levels of prestress (full line: zero prestress, dots: 10 MPa of prestress).

In addition to the principal values of the second order damage tensor,  $\mathbf{D}$ , we propose to also consider a scalar measure of damage related to the overall cracks density parameter,  $d = \sum_{r=1}^N \omega^r d^r$  (see Fig. 2). It appears that the damage amount and evolution are affected by  $\sigma_0$ . The higher is the prestress  $\sigma_0$ , the earlier damage occurs under tensile loading. In all cases, damage is about three times higher in loading direction (axial direction) than in the perpendicular direction to loading (radial direction). Note that due to the symmetry of the loading (uniaxial tensile loading path),  $D_{22} = D_{11}$ ,  $D_{12} = D_{21} = D_{13} = D_{31} = D_{23} = D_{32} = 0$ . As in [28], such anisotropy can also be illustrated by a rosette diagram which represents cracks density parameter as function of the orientations of the normals to microcracks (see Fig. 3). These surfaces appear to be distorted and admit maximum values along the  $z$ -axis. This means that microcracks are strongly developed in a plane perpendicular to the loading axis  $z$ , i.e. in  $(x,y)$  plane. Furthermore, at a given stress level, microcracks orientational distribution seems to be homothetic for the three considered pre-stresses: the higher is the prestress, the smaller is the damage amount at a same loading. However, at failure (numerically associated to the loss of convergence of the computations), all the cracks orientation distributions are similar, irrespective of the prestress. This suggests that failure may be controlled by the damage amount.

We present now the study of the effects of microcracks closure on the macroscopic behavior. To this end, consider uniaxial tension followed by unloading and reloading in uniaxial compression. The objective is to evaluate how the closure of open microcracks generated during the tension loading affects the material response during the compression phase. Note that the response under tension loading is the same as described previously. The obtained stress–strain curves for different values of the initial stresses, reported in Fig. 4, show continuous responses at the tension–compression transition (at  $\Sigma = 0$  which corresponds to the microcracks closure) despite the discontinuity of the homogenized elastic properties. Indeed, it is observed that a partial recovery of Young's modulus in the load direction is obtained (see Fig. 5); this is due to the fact that

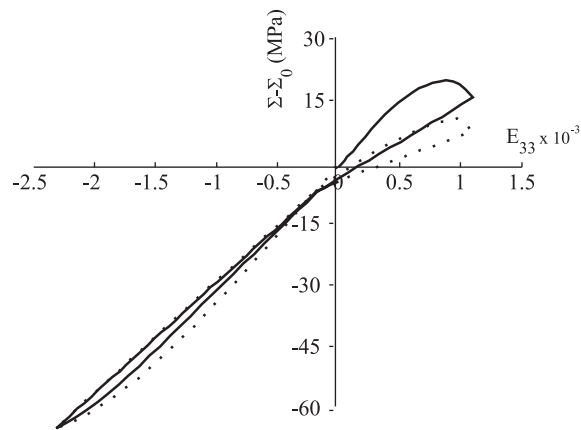


**Fig. 7.** Comparison of the responses according to the dilute scheme-based model for uniaxial loading for 10 MPa of prestress (full line: traction–compression loading, dots: compression–traction loading).

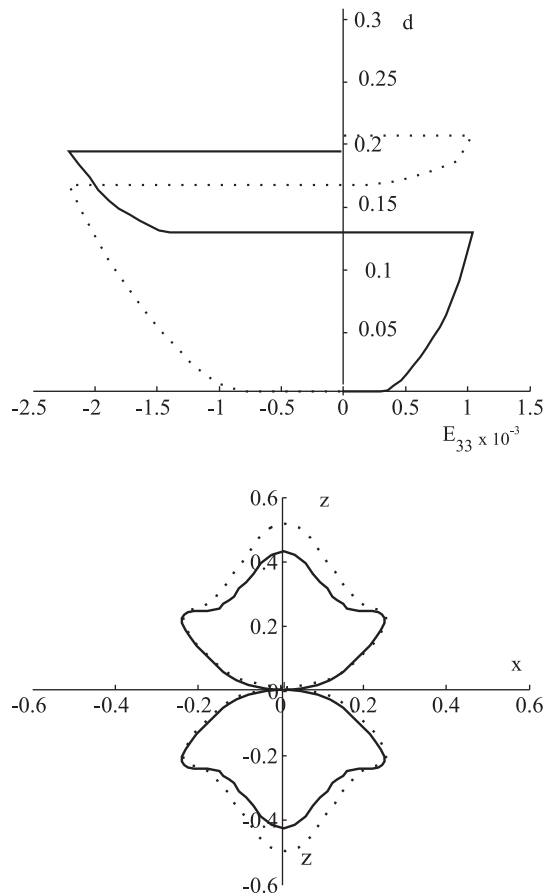


**Fig. 8.** Comparison of the damage and of the damage orientational distribution according to the dilute scheme-based model for uniaxial loading (along  $z$ -axis) for 10 MPa of prestress (full line: traction–compression loading, dots: compression–traction loading).

cracks which are not normal to the loading direction still contribute to this Young's modulus. In the tensile loading phase, for the same value of axial deformation, the damage is slightly higher for the initial stress  $\sigma_0 = 10$  MPa. Just after the tensile load peak, this increase seems to be more important. In contrast, at the end of the second loading phase (compression) the amount of damage is less important for the same prestress  $\sigma_0 = 10$  MPa.

Microcracks orientational distribution after tension followed by compression loading and then unloading is depicted on Fig. 6. A significant difference is observed when comparing to the case of only tension followed by complete unloading. This is mainly due to the occurrence of shear cracks during the compression loading phase.

Alternatively, it can be interesting to apply first compressive loading and then unloading and reloading in tension. It is expected that this macroscopic loading path generates first closed shear-like microcracks which will be reopened during tension reloading. The interest of this simulation is:

- to assess how the traction (positive) prestress affects the response in the subsequent with a first compressive loading phase.
- to demonstrate the continuity of the mechanical response during the transition from closure to opening of diffuse microcracks.

The material response corresponding to the above loading path is shown in Fig. 7 and compared with the tension followed by compression loading path response. It is observed that the mechanical responses are completely different in these two cases. Representation of the corresponding damage (see Fig. 8) shows that the material is highly deteriorated in the case when the compression loading path is first applied.

### 5. Approximate anisotropic damage model in presence of initial stress and connection with an existing macroscopic model

It is now interesting to discuss and compare the proposed damage model to existing macroscopic ones dealing with residual stresses. In particular, the anisotropic model formulated by Halm and Dragon [9] will be considered in the following.

To this end, a first step consists to restrict our model to the case where anisotropic damage can be suitably represented by a second order tensor. For this, we take advantage of approximations already used by Lubarda and Krajcinovic [17] (see also Thikhomirov et al. [26], Qiang et al. [25] and Pensée [22]).

#### 5.1. Anisotropic damage representation by means of a second order tensor $\mathbf{D}$

Following [17], the continuous distribution of microcracks density parameter, denoted here  $d(\underline{n})$ , can be described by a second order tensor  $\boldsymbol{\rho}$  such as  $d(\underline{n}) = \boldsymbol{\rho} : (\underline{n} \otimes \underline{n})$ . Vector  $\underline{n}$  represents the unit normal to a considered microcracks family. Tensor  $\boldsymbol{\rho}$  can be expressed as a function of the macroscopic variable  $\mathbf{D}$  (of Eq. (27)) in the form:

$$\boldsymbol{\rho} = \frac{15}{2} (\mathbf{D} - \frac{1}{5} \text{tr}(\mathbf{D}) \boldsymbol{\delta}) \quad (29)$$

So:

$$d(\underline{n}) = \frac{15}{2} (\mathbf{D} : (\underline{n} \otimes \underline{n}) - \frac{1}{5} \text{tr}(\mathbf{D})) \quad (30)$$

#### 5.2. Expression of the energy potential based on the damage tensor $\mathbf{D}$

We aim now at formulating the macroscopic energy potential  $\Psi$  as function of  $\mathbf{D}$ . To this end, (13) together with (14) has to be considered for the case of a continuous distribution of microcracks. It is thus required the replacement of summation by an integration on the surface of unit sphere, that is over all the orientations in space. It is then necessary to compute the quantity

$$\mathbb{D} = \frac{1}{4\pi} \int_{S^2} d(\underline{n}) (\underline{n} \otimes \underline{n} \otimes \underline{n} \otimes \underline{n}) dS \quad (31)$$

By reporting  $d(\underline{n})$  given by (30) in the above integral, it follows that:

$$\mathbb{D} = \frac{15}{8\pi} \mathbf{D} : \int_{S^2} (\underline{n} \otimes \underline{n} \otimes \underline{n} \otimes \underline{n} \otimes \underline{n} \otimes \underline{n}) dS - \frac{\text{tr} \mathbf{D}}{20} \int_{S^2} (\underline{n} \otimes \underline{n} \otimes \underline{n} \otimes \underline{n}) dS \quad (32)$$

Using now the following identities reported in [10] (see also [25])

$$\frac{1}{4\pi} \int_{S^2} n_i n_j n_k n_l n_x n_y n_z dS = \frac{1}{7} \left\{ \begin{array}{l} \delta_{ij} R_{klz\beta} + \delta_{ik} R_{jltz\beta} + \delta_{il} R_{jkz\beta} \\ + \delta_{ix} R_{jkl\beta} + \delta_{iy} R_{jklz} \end{array} \right\} \quad (33)$$

where  $R_{ijkl}$  are the components of  $\mathbb{R} = \int_{S^2} (\underline{n} \otimes \underline{n} \otimes \underline{n} \otimes \underline{n}) dS = \frac{1}{3} \mathbb{J} + \frac{2}{15} \mathbb{K}$ , we obtain that:

$$\mathbb{D} = \frac{1}{4\pi} \int_{S^2} d(\underline{n}) (\underline{n} \otimes \underline{n} \otimes \underline{n} \otimes \underline{n}) dS = \frac{1}{7} \left\{ -\frac{3}{5} (\text{tr} \mathbf{D}) \mathbb{R} + (\boldsymbol{\delta} \otimes \mathbf{D} + \mathbf{D} \otimes \boldsymbol{\delta}) + 2(\boldsymbol{\delta} \otimes \mathbf{D} + \mathbf{D} \otimes \boldsymbol{\delta}) \right\} \quad (34)$$

We are ready now for the replacement of summation in (13) by the integration on the surface of unit sphere. For simplicity, only opened microcracks are considered here. Taking into account (27) and (34), the integration procedure leads to the following closed-form expression of the macroscopic energy potential in presence of initial stress  $\sigma_0$ :

$$\begin{aligned} \Psi(\mathbf{E}, \mathbf{D}) = & \frac{1}{2} \mathbf{E} : \mathbb{C}^s : \mathbf{E} + \alpha' \text{trEtr}(\mathbf{E} \cdot \mathbf{D}) + 2\beta' \text{tr}(\mathbf{E} \cdot \mathbf{E} \cdot \mathbf{D}) + \text{trD}[\gamma'(\text{trE})^2 + \chi' \text{tr}(\mathbf{E} \cdot \mathbf{E})] + \text{tr}(\sigma_0 \cdot \mathbf{E}) \\ & - \frac{16}{3}(1 - \nu^s) \left[ \frac{\nu^s}{1 - 2\nu^s} \text{trEtr}(\sigma_0 \cdot \mathbf{D}) + \frac{2}{2 - \nu^s} \text{tr}(\sigma_0 \cdot \mathbf{D} \cdot \mathbf{E}) \right. \\ & \left. - \frac{\nu^s}{2 - \nu^s} \left[ -\frac{1}{35} \text{trD}(\text{trEtr}\sigma_0 + 2\text{tr}(\sigma_0 \cdot \mathbf{E})) + \frac{1}{7} \text{trEtr}(\sigma_0 \cdot \mathbf{D}) + \frac{1}{7} \text{tr}\sigma_0(\text{trE} \cdot \mathbf{D}) + \frac{2}{7} \text{tr}(\sigma_0 \cdot \mathbf{E} \cdot \mathbf{D}) + \frac{2}{7} \text{tr}(\sigma_0 \cdot \mathbf{D} \cdot \mathbf{E}) \right] \right] \end{aligned} \quad (35)$$

with

$$\alpha' = -a_1 \nu^s \left( \frac{2 - \nu^s}{1 - 2\nu^s} - \frac{1}{7} \right) \quad (36)$$

$$2\beta' = -a_1 \left( 1 - \frac{2}{7} \nu^s \right) \quad (37)$$

$$\gamma' = -a_1 \frac{\nu^s}{2} \left( \frac{(2 - \nu^s)\nu^s}{(1 - 2\nu^s)^2} + \frac{\nu^s}{35} \right) \quad (38)$$

$$\chi' = -a_1 \frac{\nu^s}{35} \quad (39)$$

in which  $a_1 = \frac{16E^s(1-\nu^s)}{3(2-\nu^s)(1+\nu^s)}$ .

Expression (35) can be rewritten as:

$$\begin{aligned} \Psi(\mathbf{E}, \mathbf{D}) = & \frac{1}{2} \mathbf{E} : \mathbb{C}^s : \mathbf{E} + \alpha' \text{trEtr}(\mathbf{E} \cdot \mathbf{D}) + 2\beta' \text{tr}(\mathbf{E} \cdot \mathbf{E} \cdot \mathbf{D}) + \text{trD} \left[ \gamma'(\text{trE})^2 + \chi' \text{tr}(\mathbf{E} \cdot \mathbf{E}) \right] + \text{tr}(\sigma_0 \cdot \mathbf{E}) \\ & - \frac{16}{3}(1 - \nu^s) \left[ \frac{(13 - 5\nu^s)\nu^s}{7(1 - 2\nu^s)(2 - \nu^s)} \text{trEtr}(\sigma_0 \cdot \mathbf{D}) + \frac{7 - 2\nu^s}{7(2 - \nu^s)} \text{tr}(\sigma_0 \cdot \mathbf{D} \cdot \mathbf{E}) \right. \\ & \left. - \frac{\nu^s}{2 - \nu^s} \left[ -\frac{1}{35} \text{trD}(\text{trEtr}\sigma_0 + 2\text{tr}(\sigma_0 \cdot \mathbf{E})) + \frac{1}{7} \text{tr}\sigma_0(\text{trE} \cdot \mathbf{D}) \right] \right] \end{aligned} \quad (40)$$

It is worth noticing that this expression depends linearly or quadratically on  $\mathbf{E}$ , and linearly on  $\mathbf{D}$  and  $\sigma_0$ , through their invariants or mixed invariants.

### 5.3. Link with an existing macroscopic damage model including residual stress

The macroscopic thermodynamic potential derived in this paper (Eq. (35)) is now compared to the potential already proposed by [9] who considered also the effects of residual stresses in the context of a macroscopic anisotropic damage model. Using the notations introduced by these authors, the model [9] corresponds to the following energy potential:

$$\Psi^{HD} = \frac{1}{2} \mathbf{E} : \mathbb{C}^s : \mathbf{E} + \alpha \text{trEtr}(\mathbf{E} \cdot \mathbf{D}) + 2\beta \text{tr}(\mathbf{E} \cdot \mathbf{E} \cdot \mathbf{D}) + g \text{tr}(\mathbf{E} \cdot \mathbf{D}) \quad (41)$$

where  $\alpha$  and  $\beta$ , similar to  $\alpha'$  and  $\beta'$  in (35), are now two material parameters to be identified and the term  $g \text{tr}(\mathbf{E} \cdot \mathbf{D})$  represents the effect of a residual stress  $g\mathbf{1}$ . Clearly enough, the model proposed by these authors corresponds to a spherical initial stress for which (35) reads (with  $\sigma_0 = g\mathbf{1}$ ):

$$\begin{aligned} \Psi(\mathbf{E}, \mathbf{D}) = & \frac{1}{2} \mathbf{E} : \mathbb{C}^s : \mathbf{E} + \alpha' \text{trEtr}(\mathbf{E} \cdot \mathbf{D}) + 2\beta' \text{tr}(\mathbf{E} \cdot \mathbf{E} \cdot \mathbf{D}) + \text{trD}[\gamma'(\text{trE})^2 + \chi' \text{tr}(\mathbf{E} \cdot \mathbf{E})] + g' \text{trE} \\ & - \frac{16}{3} \frac{\nu^s(1 - \nu^s)}{1 - 2\nu^s} g' \text{trDtrE} - \frac{16}{3} (1 - \nu^s) g' \text{tr}(\mathbf{E} \cdot \mathbf{D}) \end{aligned} \quad (42)$$

Comparison between Eqs. (42) and (41) shows that, in absence of initial stress, the two scale approach model proposed in this paper accounts for the contribution of the isotropic part of the damage tensor, namely  $\text{trD}[\gamma'(\text{trE})^2 + \chi' \text{tr}(\mathbf{E} \cdot \mathbf{E})]$ , which does not appear in the model of [9]. Concerning the effect of the initial stress ( $g$  or  $g'$ ), both models capture its influence through the term of  $\text{tr}(\mathbf{E} \cdot \mathbf{D})$ . However, in addition to this term, the two scale approach accounts for supplementary effects given by  $g' \text{trDtrE}$ . It is convenient to note also the presence in the two scale model of the quantity  $g' \text{trE}$ , which obviously accounts for the prestress effect in absence of damage.

It is worth noticing that the expression (42) for the energy potential can be derived from representation theorems for tensor functions (see for instance [4]) which constitute a rigorous way to derive purely macroscopic models that automatically satisfy the material symmetries associated or induced by different agencies (e.g. damage). One advantage of the present micromechanical derivation over the representation theorems is that, except for the elastic coefficients of the solid matrix, it does not require any damage constant to be identified.

## 6. Conclusion

In this study, we have proposed a new anisotropic damage model taking into account an initial stress  $\sigma_0$ . The micromechanical approach used is based on a careful analysis (in the context of Eshelby-like homogenization methods) of microcracked media in presence of the initial stress. Cracks closure effects are also incorporated in the model. Taking advantage of the dilute concentration assumption, a closed-form formulation is provided. In particular, the effects of the initial stress are fully detailed. Moreover, the rate form of the constitutive anisotropic damage is reported. For illustration purposes, the proposed model has been implemented and applied for different values of  $\sigma_0$  and for various loading paths. It is shown that  $\sigma_0$  strongly affects the damage orientational distribution and subsequently the macroscopic response of the material. Interestingly, in the case when the orientational distribution of microcracks density parameter is approximated by means of a second order damage tensor  $\mathbf{D}$ , a connection is established between the present model and the macroscopic one proposed by Halm and Dragon [9]. Obviously the present model can be extended by considering other homogenization schemes (Mori–Tanaka, Ponte-Castaneda and Willis bound) as recently analyzed in the context of unilateral behavior of cracked media by Dormieux and Kondo [6]. This is out of the scope of the present study.

## References

- [1] Andrieux S, Bamberger Y, Marigo J-J. Un modèle de matériaux microfissuré pour les roches et les bétons. *J Méca Théor Appl* 1986;5:471–513.
- [2] Barthélémy J-F, Dormieux L. A micromechanical approach to the strength criterion of Drucker–Prager materials reinforced by rigid inclusions. *Int J Numer Anal Methods Geomech* 2004;28:565–82.
- [3] Bazant ZP, Oh BH. Efficient numerical integration on the surface of a sphere. *ZAMM* 1986;66:37–49.
- [4] Boehler JP. CISM courses and lectures, chapter application of tensors functions in solids mechanics. Springer; 1987.
- [5] Budiansky B, O’Connell R. Elastic moduli of a cracked solid. *Int J Solids Struct* 1976;12:81–97.
- [6] Dormieux L, Kondo D. Stress-based estimates and bounds of effective elastic properties: the case of cracked media with unilateral effects. *Comput Mater Sci* 2009;46:173–9.
- [7] Dormieux L, Kondo D, Ulm F-J. *Microporomechanics*. Wiley; 2006.
- [8] Dormieux L, Molinari A, Kondo D. Micromechanical approach to the behavior of poroelastic materials. *J Mech Phys Solids* 2001;50:2203–31.
- [9] Halm D, Dragon A. A model of anisotropic damage by mesocrack growth: unilateral effect. *Int J Damage Mech* 1996;5:384–402.
- [10] He Q-C, Curnier A. A more fundamental approach to damaged elastic stress–strain relations. *Int J Solids Struct* 1995;32:1453–7.
- [11] Horii H, Nemat-Nasser S. Overall moduli of solids with microcracks : load-induced anisotropy. *J Mech Phys Solids* 1983;31:155–71.
- [12] Krajcinovic D. *Damage mechanics*. North-Holland; 1996.
- [13] Laws N. On the thermostatics of composite materials. *J Mech Phys Solids* 1973;21:9–17.
- [14] Lennon AB, Prendergast PJ. Residual stress due to curing can initiate damage in porous bone cement: experimental and theoretical evidence. *J Biomech* 2002;35:311–21.
- [15] Levasseur S, Collin F, Charlier R, Kondo D. On a class of micromechanical damage models with initial stresses for geomaterials. *Mech Res Commun* 2010;37:38–41.
- [16] Levin VM. Thermal expansion coefficient of heterogeneous materials. *Mekh Tverd Tela* 1967;2:83–94.
- [17] Lubarda VA, Krajcinovic D. Damage tensors and the crack density distribution. *Int J Solids Struct* 1993;30:2859–77.
- [18] Maghous S, Dormieux L, Barthélémy J-F. Micromechanical approach to the strength properties of frictional geomaterials. *Eur J Mech A/Solids* 2009;28:188–99.
- [19] Marigo J-J. Modeling of brittle and fatigue damage for elastic material by growth of microvoids. *Engng Fract Mech* 1985;21(4):861–74.
- [20] Mura T. *Micromechanics of defects in solids*. 2nd ed. Martinus Nijhoff Publ.; 1987.
- [21] Murakami S, Kamiya K. Constitutive and damage evolution equations of elastic brittle materials based on irreversible thermodynamics. *Int J Mech Sci* 1997;39(4):473–86.
- [22] V. Pensée. Contribution de la micromécanique à la modélisation tridimensionnelle de l’endommagement par mésolfissuration. PhD thesis, Université des Sciences et Technologies de Lille; 2002.
- [23] Pensée V, Kondo D. Une analyse micromécanique 3-d de l’endommagement par mésolfissuration. *CR Acad Sci – Sér IIb – Méc* 2001;329:271–6.
- [24] Pensée V, Kondo D, Dormieux L. Micromechanical analysis of anisotropic damage in brittle materials. *J Engng Mech* 2002;128:889–97.
- [25] Qiang Y, Zhongkui L, Tham LG. An explicit expression of the second-order fabric tensor dependent elastic compliance tensor. *Mech Res Commun* 2001;28:255–66.
- [26] Thikomirov D, Niekamp R, Stein E. On three-dimensional microcrack density distribution. *ZAMM* 2001;81:3–16.
- [27] Zhu Q, Shao JF, Kondo D. A micromechanics-based non-local anisotropic model for unilateral damage in brittle materials. *CR Méc* 2008;336:320–8.
- [28] Zhu QZ, Kondo D, Shao JF. Homogenization-based analysis of anisotropic damage in brittle materials with unilateral effect and interactions between microcracks. *Int J Numer Anal Methods Geomech* 2009;33:749–72.